

Measurement of the radiation from thermal and nonthermal radio sources

Preethi Pratap

MIT Haystack Observatory, Westford, Massachusetts 01886

Gordon McIntosh

Division of Science and Mathematics, University of Minnesota, Morris, Minnesota 56267

(Received 1 April 2004; accepted 17 December 2004)

The widespread use of the internet has enabled complex instrumentation to be available remotely and made it possible for students to use facilities to which they might otherwise not have access. Internet access to radio astronomical observatories, including the 37 m radio telescope at the Massachusetts Institute of Technology Haystack Observatory, has opened up new possibilities for undergraduate laboratory activities and research. This capability allows undergraduates to acquire and analyze radio astronomical data and investigate astrophysical systems that cannot be investigated using optical telescopes. We describe a radio astronomical activity using the spectral index to investigate the difference between thermal and nonthermal radiation and the sources that emit these forms of radiation. © 2005 American Association of Physics Teachers.

[DOI: 10.1119/1.1858485]

I. INTRODUCTION

In the past 50 years many discoveries have been made with radio telescopes that have illustrated the need for multi-wavelength observations of the universe. Radio waves also are one of the most accessible parts of the electromagnetic spectrum from the surface of the Earth. The radio-frequency range is arbitrarily defined to be from supersonic frequencies beginning at about 20 kHz, up to about 600 GHz, where the far infrared begins. The Earth's atmosphere is quite transparent in a radio window from 100 MHz to 100 GHz.¹

Until recently, most of the laboratory activities and research projects at the undergraduate and pre-college levels have emphasized the optical part of the spectrum. However, in the last ten years this emphasis has begun to change. The undergraduate education program at the MIT Haystack Observatory has focused on bringing radio astronomy into the undergraduate classroom.

The 37 m telescope that is used for the project discussed in this paper is remotely accessible to students anywhere in the world. Complex instrumentation that is available remotely introduces students to facilities that they otherwise would not be able to use.

Several recent studies have indicated the importance of research and inquiry based education at all levels.^{2,3} The Boyer report² strongly suggested that research-based learning is necessary to teach science, technology, engineering, and mathematics effectively. Providing teachers, especially those at small colleges that have limited resources, with the means of incorporating research into their teaching is an important goal of our program. The project described in this paper uses a research grade instrument in a hands-on, laboratory experience.

A discussion of thermal (blackbody) radiation and nonthermal radiation is included in many physics and astronomy courses. Although distinct forms of radiation are described in courses and texts in astronomy,^{1,4–6} radio astronomy,^{7,8} astrophysics,⁹ modern physics,¹⁰ and electromagnetic theory,¹¹ there are few, if any, measurements that can be made by undergraduates to differentiate between these two forms of radiation. The availability of the 37 m Haystack Radio Telescope to observe and study thermal and nonther-

mal radiation makes it possible to experimentally investigate this topic in undergraduate physics and astronomy classes. This paper describes the basic theory of thermal and nonthermal radiation mechanisms in the radio range of the electromagnetic spectrum. Activities are presented that describe the measurement of the spectral index, which is the frequency dependence of thermal and nonthermal radiation, for specific sources. The spectral index is then used to differentiate between various radiation mechanisms.

II. THE 37 M HAYSTACK RADIO TELESCOPE

The radio telescope at the MIT Haystack Observatory is a parabolic antenna of 37 m diameter enclosed in a radome, which protects the antenna from the weather.¹² The radome consists of a material similar to Teflon, chosen because of its strength and transparency at radio wavelengths, stretched over a semirandom strut structure used for support. The struts are arranged in a semirandom configuration to avoid periodic signals, such as reflections caused by the metal struts, which could mimic a real signal. The antenna configuration is Cassegrainian with a deformable secondary reflector at the prime focus which provides focus, tilt, and translational motion under computer control for feed offsets and focus. Two radiometers spanning the frequency ranges 21–25 GHz and 36–49 GHz are available to students. The radiometer systems detect and amplify the received signals. The signals are then processed to determine the power received at various frequencies. The frequency channels can be as small as 0.66 MHz to study spectral line sources or as large as 160 MHz to study continuum sources. The frequency resolution is under the control of the observer. The frequency ranges of the radiometers provide access to the emission from hydrogen recombination lines,¹³ several molecules in interstellar gas (for example, water, ammonia, methanol, silicon monoxide), as well as information about continuum thermal and nonthermal radio emission from a variety of astronomical sources.

With relatively little effort students can access the telescope and perform sophisticated observation projects. Resources to monitor the telescope performance and a near-real time video of the actual instrument are available. All the

information that is available to a user sitting at the console at the Haystack site is available to a user on a computer at a remote site.

III. EMISSION FROM RADIO SOURCES

The measurement technique for each of the windows in the electromagnetic spectrum is different and leads to the categorization of the different branches of astronomy such as radio, infrared, optical, x-ray, and gamma ray. In addition to the different technologies that drive the different branches of astronomy, the emissions from different astronomical sources in the various windows are different. For example, diffuse, cool gas can be detected because it emits or absorbs the hyperfine structure line of the hydrogen atom at $\lambda = 21$ cm; this gas cannot be detected by any other means. Intense and extended jets of emission from the black holes at the centers of galaxies are most apparent in radio continuum observations. Observations from each of the spectral windows gives valuable information about the nature of the astronomical source.

Astrophysical radio sources can be classified into those that radiate by thermal mechanisms and those that radiate by nonthermal mechanisms. These sources of radiation can be further subdivided into sources that produce a continuous spectrum and those that produce spectral lines. In radio astronomy, thermal spectral lines are those arising from a population distribution of energy levels that is in local thermodynamic equilibrium with the gas in the cloud. Nonthermal emission from molecules comes from population inversion, which results in maser emission. Because the activities described in this paper deal with continuum sources, we refer interested readers to Ref. 6 and references therein for further discussion on molecular emission physics.

A radio telescope measures the power from an astronomical source. Because this power varies over a solid angle in the sky, radio astronomers use a quantity called the flux density to denote the emission from a source in the sky. The flux density is defined as the power received from a radio astronomical source per unit frequency per unit area; it has units of Janskys (Jy), and is indicated by the symbol S_ν . One Jansky is $10^{-26} \text{ W m}^{-2} \text{ Hz}^{-1}$. The subscript ν indicates that S is a function of frequency.

The variation of the flux density with frequency is characterized by the spectral index s . The relation between the flux density and the frequency is given by

$$S_\nu \propto \nu^s. \quad (1)$$

The spectral index of radio sources is different for thermal and nonthermal sources. For thermal sources, the flux density of the source increases or stays relatively constant (when the source is ionized) with increasing frequency. Nonthermal sources are more intense at lower frequencies. In Fig. 1, 3C273 (a quasar), Cas A (a supernova remnant), and Cygnus A (a radio galaxy) are examples of nonthermal sources, while the quiet Sun⁶ and the Moon are examples of thermal sources.

IV. THERMAL EMISSION FROM RADIO SOURCES

All objects that are at nonzero temperatures emit energy in the form of electromagnetic radiation. Not only do these objects radiate electromagnetic energy, they also absorb the energy. A perfect absorber (or radiator) is called a blackbody.

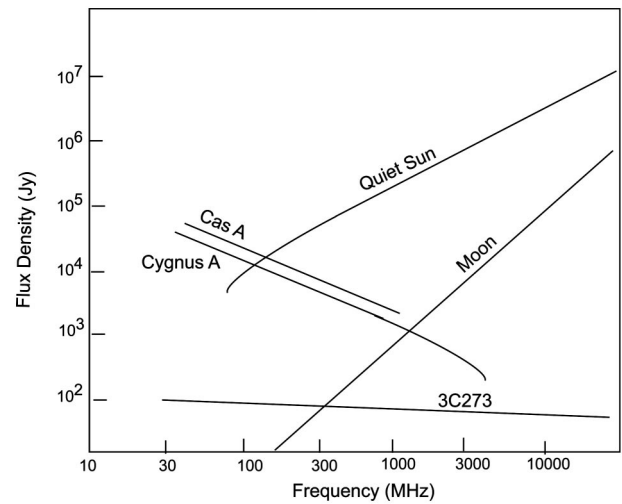


Fig. 1. The frequency spectra of several astronomical sources. The quiet Sun (see Ref. 6) and the Moon are examples of thermal sources, while Cas A, Cygnus A and 3C273 are examples of nonthermal sources.

The emission from a perfect blackbody is solely determined by its temperature and is a function of frequency. Although no astronomical objects are perfect blackbodies, this assumption adequately describes thermal emission from many radio sources.

The frequency distribution of blackbody radiation is described by the Planck function

$$B(\nu) = \frac{2h\nu^3}{c^2} \frac{1}{e^{h\nu/kT} - 1}, \quad (2)$$

where $B(\nu)$, known as the brightness, is in units of watts $\text{m}^{-2} \text{ Hz}^{-1} \text{ rad}^{-2}$, h is Planck's constant, c is the velocity of light, k is Boltzmann's constant, and T is the thermodynamic temperature. For radio astronomical purposes the Rayleigh–Jeans approximation of low photon energy compared to the thermal energy, $h\nu \ll kT$, can be used. This approximation is presented in various texts as background in the development of the Planck function.^{7,14} (A calculation of the accuracy of this approximation could be included in an observing activity based on this paper.) The Rayleigh–Jeans approximation accurately describes thermal radio emission and is used throughout this region of the electromagnetic spectrum. In this approximation the Planck function can be written as

$$B(\nu) = \frac{2\nu^2 kT}{c^2}. \quad (3)$$

Equation (3) can be used to define the brightness temperature, T_b , which is defined as the Rayleigh–Jeans temperature of an equivalent blackbody that has the same power per unit area per unit frequency per unit solid angle as the astronomical source

$$T_b = \frac{c^2}{2k} \frac{B(\nu)}{\nu^2}. \quad (4)$$

For a solid body such as a planet, Eq. (4) describes the observed brightness temperature, and the thermodynamic temperature and the brightness temperature are equal.

V. DETECTION OF RADIO EMISSION

The radio telescope receives radiation in a solid angle that is called the beam of the antenna. The resolution or beam-width (θ) of a telescope is determined by diffraction theory to be

$$\theta = \frac{1.22\lambda}{D}, \quad (5)$$

where λ is the observed wavelength and D is the diameter of the telescope. (A calculation of the resolution of the telescope at the appropriate frequencies could be included as another activity.) The radiation detected by the radio telescope is generally given in terms of the antenna temperature, T_A , which is the temperature of a resistor that would generate the same power per frequency interval at its terminals as the observed source in a specified frequency range. If we assume a constant source brightness and an accurately pointed antenna, we have for a discrete source (small compared to the antenna beam)

$$T_A = T_b \frac{\Omega_S}{\Omega_A}, \quad (6)$$

where Ω_S is the solid angle subtended by the source and Ω_A is the size of the solid angle of the beam. (Planets are discrete sources for the Haystack telescope. A comparison of the angular size of the telescope beam and the observed planet should be included as a related activity.) The flux density is calculated using the measured antenna temperature, T_A , according to

$$S_\nu = \frac{2kT_A}{\eta_{\text{eff}}A}, \quad (7)$$

where η_{eff} , the aperture efficiency, is the ratio of the effective aperture to the physical aperture, A . From Eqs. (3), (5), (7), and $\eta_{\text{eff}}A = c^2/(\nu^2\Omega_A)$ (Ref. 5, Chap. 6), we have for a discrete source

$$S_\nu = \frac{2kT_b\nu^2\Omega_S}{c^2}, \quad (8)$$

which implies from Eq. (7) that

$$\frac{T_A}{\eta_{\text{eff}}A} = \frac{T_b\nu^2\Omega_S}{c^2}. \quad (9)$$

Because for the same blackbody source the temperature and size are constant and the antenna aperture is constant, we have

$$S_\nu \propto \frac{T_A}{\eta_{\text{eff}}} \propto \nu^2. \quad (10)$$

Thus, the spectral index for a blackbody, as defined in Eq. (1), is two.¹⁵ From Eq. (10) the spectral index can be determined from the flux density of the source at two frequencies

$$\frac{S_{\nu_1}}{S_{\nu_2}} \propto \left(\frac{T_{A,1}}{\eta_{\text{eff},1}} \right) \left(\frac{\eta_{\text{eff},2}}{T_{A,2}} \right) \propto \left(\frac{\nu_1}{\nu_2} \right)^{-2}. \quad (11)$$

The subscripts 1 and 2 indicate measurements at frequencies 1 and 2, respectively.

VI. NONTHERMAL EMISSION FROM RADIO SOURCES

Theoretically many different radiation mechanisms can be responsible for nonthermal emission from radio sources. In practice, nonthermal radio sources are dominated by synchrotron emission. Examples of such sources are supernova remnants and active galactic nuclei. Radio emission occurs when relativistic electrons spiral around a weak magnetic field.⁸ A synchrotron spectrum is usually approximated by a power law over a limited range of frequencies. The spectral index for this radiation can be defined as $s = (1 - p)/2$, where p characterizes the power law distribution of the relativistic electrons or, explicitly, the distribution of relativistic electrons $N(E) \propto E^{-p}$. Most nonthermal radio sources have spectral indices between -0.5 and -1.5 , corresponding to values of p between 2 and 4. Again the spectral index can be determined by taking the ratio of the flux density at two frequencies.

VII. MEASURING THE SPECTRAL INDEX OF A THERMAL SOURCE WITH THE HAYSTACK TELESCOPE

In an experiment performed with the 37 m telescope, students calculate the fluxes of two planets at two different frequencies by measuring the antenna temperature, T_A . These quantities are used with an assumed aperture efficiency in Eq. (7). The 37 m telescope has receivers at the 21–25 GHz frequency range and at the 36–49 GHz frequency range. Students calculate the fluxes of the planets at the frequencies in the two bands to obtain the spectral index of the planet, which can then be related to the blackbody nature of the spectrum.

The telescope is pointed at a planet and the receiver is tuned to an appropriate setting in the 21–25 GHz band. After ensuring that the telescope pointing is accurate, the telescope is set to scan across the planet in azimuth and elevation, a discrete source scan. The telescope moves off the source and takes 1 s integrations across the planet. The software then fits Gaussians to the scans and the result is a peak temperature with an error related to the fit. This peak temperature is the raw antenna temperature of the planet as measured by the 37 m telescope. The procedure is repeated for a frequency in the 36–49 GHz band. Figures 2(a) and 2(b) show the data plots from azimuth scans at 22 and 44 GHz. The spectral index calculated from the measurements shown in Fig. 2 is 1.8, which is comparable to the thermal value of 2 expected from a blackbody spectrum.

The aperture efficiency, η_{eff} in Eq. (7), is $\sim 40\%$ at 22 GHz and $\sim 25\%$ at 44 GHz. The caveat in using these assumed values is that the efficiency can vary by a few percent depending on the focus of the instrument, the thermal conditions within the radome, and the elevation of the source. The assumed value of the aperture efficiency is the largest contribution to the measurement error, although systematic errors from the receiver electronics could contribute as well.

VIII. MEASURING THE SPECTRAL INDEX OF A NONTHERMAL SOURCE

Nonthermal radio emission usually comes from extragalactic radio jets or supernova remnants. Sources observed with the 37 m telescope include the supernova remnants,

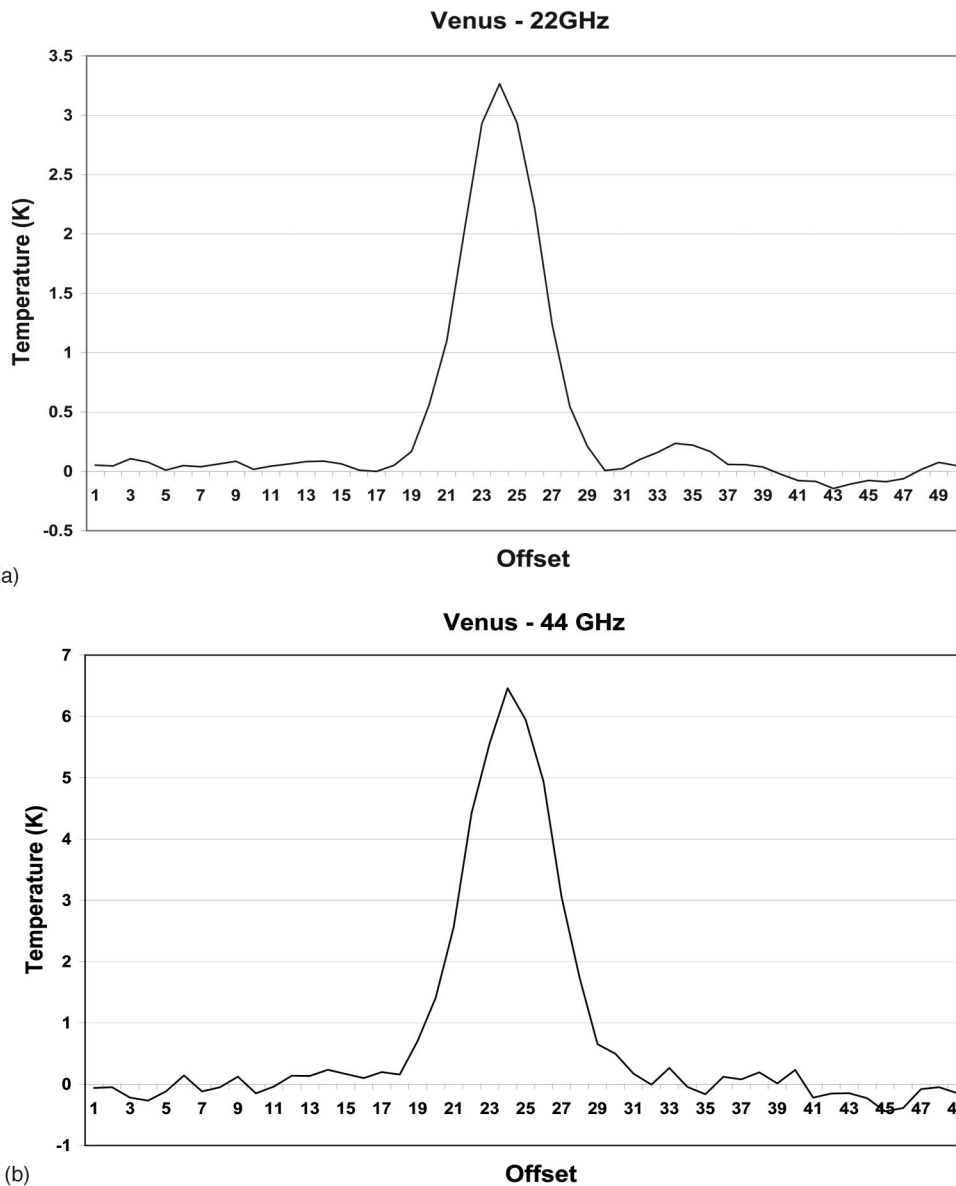


Fig. 2. (a) Plot of an azimuth scan across Venus at 22 GHz and (b) plot of an azimuth scan across Venus at 44 GHz. These plots are the results of a discrete source scan for the 37 m telescope.

Crab Nebula and Cassiopeia A, and the double lobed radio galaxy, Cygnus A. The Crab Nebula and Cygnus A are both strong sources of nonthermal radiation which can be mapped with the telescope in a short time.

The mapping technique uses a method called drift scan mapping. This technique was developed at Haystack Observatory to take into account the variations introduced by the radome enclosing the antenna. The metal struts of the radome introduce variations in the measured power, and it is impossible to determine whether these variations are a result of actual variations in the continuum emission from the source or whether they are a result of the radome structure. In the drift technique the telescope is moved ahead of the source at a given declination and made to wait while the source drifts through the beam. A map is constructed by repeating this procedure over a range of declinations that cover the source.

The drift map output is a text file which is plotted with a

PGPLOT program. This program includes identification of the peak temperature in the map, which is used in the spectral index calculations. Sample images at 21 and 41 GHz of Cygnus A are shown in Fig. 3. The raw antenna temperature obtained from the measurements is converted to a brightness temperature using the aperture efficiency.

Figure 3 also indicates the difference in the resolution at the two frequencies [see Eq. (5)]. The resolution of the observations at 44 GHz is twice the resolution of those at 22 GHz. For more accurate comparison the 44 GHz image can be convolved to the same resolution as the 22 GHz image using the plotting software. Again, the spectral index can be calculated from Figs. 3(a) and 3(b), using the values in the header. As an example, from the measurements shown in Fig. 3 the resulting spectral index is -1.2 , which is consistent with the spectral index of -1.27 for Cygnus A at frequencies above 1 GHz obtained by Mitton and Ryle.¹⁶ The

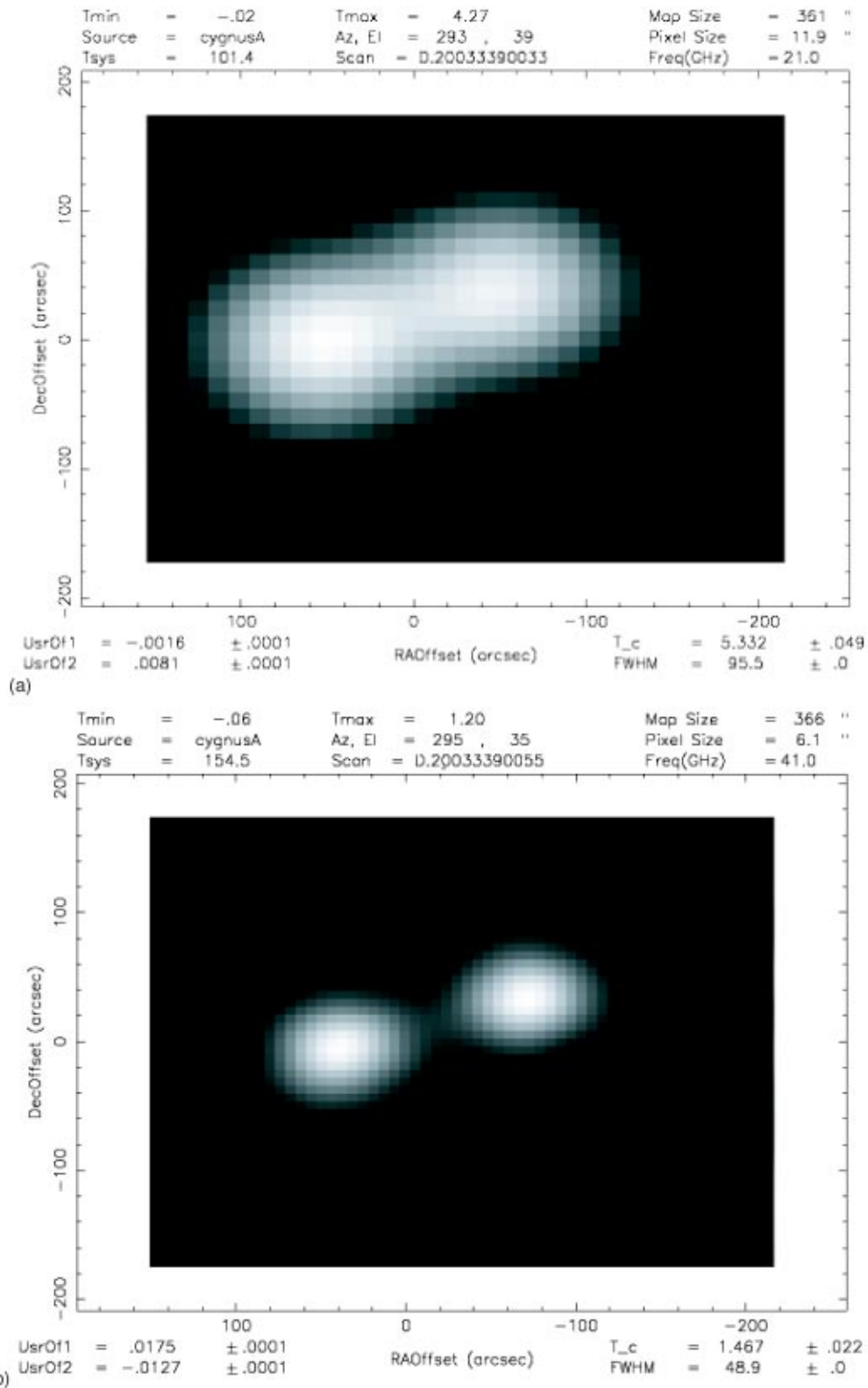


Fig. 3. Images of Cygnus A, a double lobe radio galaxy made with the 37 m telescope. (a) The result of a drift scan map at a frequency of 21 GHz. The header information is mostly irrelevant for this experiment except for the continuum peak temperature T_c shown at the bottom right and the frequency shown at the top right. (b) Same as (a) but at a frequency of 41 GHz.

spectral index of the two lobes of Cygnus A also can be determined using this technique, although additional data processing will need to be done.

As mentioned in Sec. VII, a major contributor to the error is the assumed value of the aperture efficiency. Variations in the sky conditions during the data taking pro-

cess also can cause errors. Finally, the electronics in the system contributes to systematic errors. These factors can contribute to errors of 10%–20% in the final value of the spectral index.

IX. CONCLUSION

We have discussed basic physics projects that can be performed with a 37 m research grade radio telescope. The projects introduce students to radio astronomical measurements and to the physics of thermal and synchrotron radiation. The measurement of the spectral index provides a technique for determination of the difference between thermal and nonthermal sources of radiation.

Instructors interested in acquiring observing time on the telescope are directed to contact Dr. Preethi Pratap at MIT Haystack Observatory. Details about the telescope capabilities and information on obtaining time and on observation methods and telescope control software are available.¹²

ACKNOWLEDGMENTS

Undergraduate research at MIT Haystack Observatory is funded by a grant from the Divisions of Undergraduate Education and Astronomy at the National Science Foundation (Grant No. DUE-0230495). We acknowledge useful comments from two anonymous referees.

- ¹F. A. Roger and W. J. Kaufmann III, *Universe* (Freeman, New York, 2002), 6th ed.
- ²Boyer Commission on Educating Undergraduates in the Research University, “Reinventing undergraduate education: A blueprint for America’s research universities,” (Carnegie Foundation for the Advancement of Teaching, Menlo Park, CA, 1998).
- ³National Science Foundation, “Shaping the future: New expectations for undergraduate education in science, mathematics, engineering, and technology” (NSF 96-139 Arlington, 1996).
- ⁴T. T. Arny, *Explorations: An Introduction to Astronomy* (McGraw-Hill, Boston, 2002), 3rd ed.
- ⁵E. Chaisson and S. McMillan, *Astronomy Today* (Pearson Education, Upper Saddle River, NJ, 2002), 4th ed.
- ⁶M. L. Kutner, *A Physical Perspective* (Cambridge U. P., Cambridge, 2003), 12th ed.
- ⁷J. D. Kraus, *Radio Astronomy* (Cygnus-Quasar, Powell, OH, 1986).
- ⁸K. Rohlfs and T. L. Wilson, *Tools of Radio Astronomy* (Springer, New York, 2004), 4th ed.
- ⁹D. A. Ostlie and B. W. Carroll, *An Introduction to Modern Stellar Astrophysics* (Addison-Wesley, Reading, MA, 1996).
- ¹⁰J. W. Rohlfs, *Modern Physics from A to Z* (Wiley, New York, 1994).
- ¹¹D. J. Griffiths, *Introduction to Electrodynamics* (Prentice-Hall, Upper Saddle River, NJ, 1999), 3rd ed.
- ¹²See various links at (<http://www.haystack.mit.edu>)
- ¹³G. McIntosh, “A modern physics laboratory activity: Radio astronomical observations of recombination lines,” *Am. J. Phys.* **70**(3), 285–287 (2002).
- ¹⁴J. Taylor, C. Zafiratos, and M. Dubson, *Modern Physics for Scientists and Engineers* (Prentice-Hall, Upper Saddle River, NJ, 1999), 2nd ed.
- ¹⁵See Refs. 5 or 6 for further development of these concepts.
- ¹⁶S. Mitton and M. Ryle, “High resolution observations of Cygnus A at 2.7 GHz and 5 GHz,” *Monthly Notices of the Royal Astronomical Society* **146**, 221–233 (1969).



Tone Bars. These wooden tone bars give the whole notes in an octave when they are dropped, one by one, onto a hard floor. Unlike the bars of a xylophone, these all have the same length, but have different thicknesses, with the thinner bars having the higher frequencies. When they are dropped, they flex transversely, with the nodes 22.4% of the way in from the ends. This set was made by Max Kohl of Chemnitz, Germany, and is in the Greenslade Collection. (Photograph and Notes by Thomas B. Greenslade, Jr., Kenyon College)